PHYSICAL REVIEW B VOLUME 28, NUMBER 8 15 OCTOBER 1983

Critical-point study of higher conduction bands in Si single crystal by angle-resolved photoemission

A. Kasuya and Y. Nishina
The Research Institute for Iron, Steel and Other Metals, Tohoku University, Sendai 980, Japan

T. Kobayasi
College of Medical Sciences, Tohoku University, Sendai 980, Japan
(Received 11 May 1983)

A critical-point behavior in angle-resolved photoemission has been studied in single-crystal silicon for the incident-photon-energy range from 7.1 to 8.6 eV. A sharp and highly dispersive peak is observed in the relatively broad spectrum. In the direct-optical-transition model, this peak is attributed to photoexcitation of electrons from the highest valence band to a local minimum of the fifth conduction band located in the middle of the Γ—K line. The energy value E of this local minimum relative to the top of the valence band and the magnitude of its wave vector $|\vec{k}|$ are determined to be $E=6.6\pm0.1$ eV and $|\vec{k}|=(5.6\pm0.1)\times10^7$ cm^{-1}, respectively. The experimental results are quantitatively consistent with the band-structure calculation by Nara and Kobayasi.

I. INTRODUCTION

Angle-resolved photoemission from single crystals has been studied extensively for investigating the electronic structures of solids. This experimental technique has been successfully applied to determine the energy-band dispersion for a number of metals and semiconductors.[1] Most of the investigations, however, have been carried out for materials having simple conduction-band structures.[1–4] In these special cases, the final state of the photoemission process may be regarded as free-electron-like and the angular or photon-energy dependence of the photoemission spectrum represents simply the overall dispersion of the initial state (in valence bands) along certain directions in the Brillouin zone.

Since the photoemission process involves optical transition, the spectrum depends primarily on the critical-point structure of the energy bands. In the direct optical-transition model Kane[5] has shown that the structure in the photoemission spectrum is enhanced for photoexcitation at critical points in the joint density of states. The structure is enhanced also at a critical point, if any, in the density of final states. Such a spectral dependence on the final state cannot be found in the case of an ordinary optical-absorption spectrum for a band-to-band transition. Accordingly, if the incident-photon energy is tuned to the value where the optical transition takes place at a critical point, an abrupt change in the spectrum may take place at a certain emission angle so as to conserve the component of the momentum parallel to the sample surface. This experimental technique, therefore, may be applied to determine the location and types of critical point in the energy band.

There have been very few examples of investigation in angle-resolved photoemission performed from this point of view. As for the experimental verification, the critical point study has been carried out only in metals such as Cu, Au, and Ag.[6–9] Because of the simplicity of their conduction-band structures these materials exhibit critical-point behaviors corresponding to photoexcitation only at zone boundaries.[6–8] For those materials having more complicated band structures, such as most of group-IV semiconductors and III-V and II-VI compound semiconductors, the critical point may be present at any arbitrary point in the Brillouin zone regardless of its symmetry. The analysis of the spectrum can determine the location of such general critical points, as well as their dispersions, which provide specific and essential information on the band structure.

In the present investigation the critical-point behavior in angle-resolved photoemission is studied for a single crystal of Si in the photon-energy range 7.1—8.6 eV. A sharp and highly dispersive peak is observed above a relatively broad spectrum previously reported by a number of authors.[10,11] This peak is attributed to photoexcitation of electrons from the highest valence band to a local minimum of the fifth conduction band located along the Γ—K line. The analysis yields the value of energy and wave vector of this local minimum. To the best of our knowledge this paper is the first report on the use of angle-resolved-photoemission technique to determine the position of a higher conduction-band extremum located at a general point in the Brillouin zone in any crystalline solid. It is shown that the experimental results are quantitatively consistent with the band-structure calculation of Si using a nonlocal pseudopotential given by Nara and Kobayasi.[12,13]

II. EXPERIMENTAL ARRANGEMENTS

The experimental setup consists of an ion-pumped stainless-steel vacuum chamber which is connected through a sapphire window to a Seya-Namioka-type monochromator. A hydrogen-discharge lamp combined

with this monochromator gives usable light in the energy range 7.1—8.6 eV. The photoelectrons are analyzed by a 127° cylindrical deflection analyzer which is designed to work at low electron energies. The energy resolution of this analyzer is less than 30 meV at the electron kinetic energy of 1 eV. The acceptance angle is 5° for the polar and 7° for the azimuthal. The sample is cut from a single-crystal wafer doped with boron to the resistivity range of 10 Ω cm at room temperature for the convenience of cleaning the sample surface by electrical heating. After the crystal orientation is determined by x-ray diffraction, the sample is etched in an acid solution containing one part of 38 mol% H_2O_2 and three parts of concentrated H_2SO_4. Prior to the measurement, the sample is heated to 1200 °C repeatedly in the vacuum chamber to obtain a clean surface.[14] The surface contamination is examined by Auger-electron spectroscopy. For all measurements the photoelectrons are collected at a right angle to the direction of incident-photon beam and angular dependence is measured by rotation of the sample with respect to the fixed directions of the incident beam and the photoelectron analyzer. One may disregard the dependence of transition probability on the incident-beam angle, since, for the present purpose of measurements, it cannot affect the peak position of the spectrum beyond our spectral resolution but only the overall intensity. The pressure of vacuum chamber is less than 8×10^{-8} Pa during the measurements.

III. EXPERIMENTAL RESULTS

Figure 1 shows photoemission spectra for the (111) face of Si in the photon-energy range $h\nu=7.36$—8.30 eV at room temperature. The energy E of emitted electron is defined as measured with respect to the valence-band maximum. In this energy scale the photoemission from the valence-band edge gives the maximum possible electron energy in the spectrum which is equal to the incident-photon energy. The valence-band edge is determined by extrapolating the high-energy edge of the bulk photoelectron spectrum in the manner described in Ref. 15. The uncertainty in the electron energy determined by this procedure is estimated to be less than 0.1 eV. This procedure is adopted for all measurements in order to correct for the difference in work function and band bending among samples having different crystal faces. As indicated in the figure the polar angle θ of measurement is 50° from surface normal towards $\langle 0\bar{1}1\rangle$ direction which is oriented tangential to the surface. A strong peak appears at 7.0 eV for the spectrum at $h\nu=7.75$ eV. This peak is most pronounced at this photon energy and becomes weaker and more broadened for the spectra towards both sides away from this photon energy. This peak has not been observed in the previous measurements[10,11] since it becomes pronounced only at a particular value of photon energy and, as explained in the following, at a particular range of electron-emission angle. Figure 2 shows the spectra for the (111) face measured at $\theta=50°$ from the normal towards the $\langle 11\bar{2}\rangle$ direction. No pronounced peak appears in any of the spectra. This result is consistent with the measured results in Ref. 10. These spectra are measured in the same geometry as those of Fig. 1 except that the azimuth of the sample is rotated by 30°. Figures 1 and 2, therefore, indicate that the observed peak is strongly dependent on both photon energy and angle of emission. Figure 3 shows the angular dependence of the spectrum for the (111) face measured towards the $\langle 0\bar{1}1\rangle$ direction at $h\nu=7.75$ eV. Hereafter the geometry of this measurement, for example, is referred to as "the (111)-$\langle 0\bar{1}1\rangle$ measurement." The spectra show that a pronounced peak begins to appear above $\theta\cong30°$, exhibits its maximum intensity at $\theta=60°$, and then decreases with further increase in θ. It is also noted that the peak position shifts towards lower energy as θ increases. Except for this peak the spectra ex-

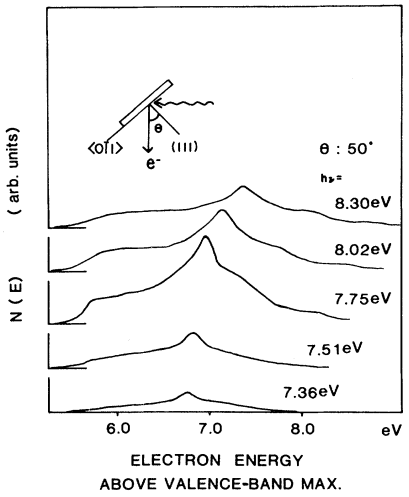

FIG. 1. Photoemission spectra for the (111) crystal face of Si in the photon-energy range 7.36—8.30 eV. Polar angle θ is set to 50° from the surface normal $\langle 111\rangle$ towards the $\langle 0\bar{1}1\rangle$ direction which is tangential to the sample surface. $N(E)$ is the number of electrons emitted with its kinetic energy E.

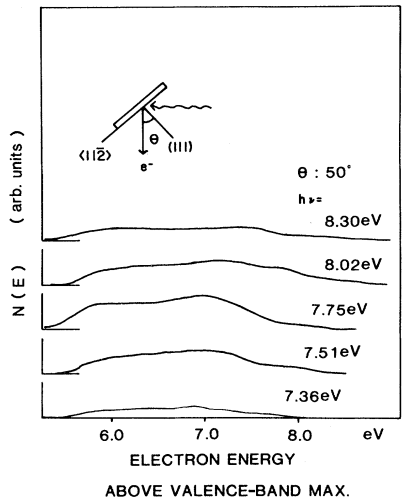

FIG. 2. Photoemission spectra for the (111) crystal face of Si in the photon-energy range 7.36—8.30 eV. Polar angle θ is set to 50° from the surface normal towards $\langle 11\bar{2}\rangle$.

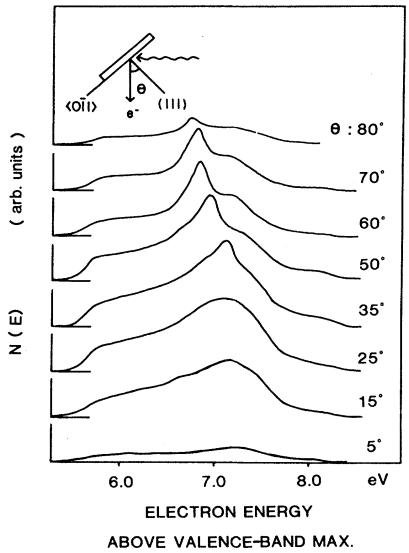

FIG. 3. Angle-resolved-photoemission spectra for the (111) crystal face of Si at $h\nu=7.75$ eV. Polar angle θ is varied from the surface normal towards the $\langle 0\bar{1}1\rangle$ direction.

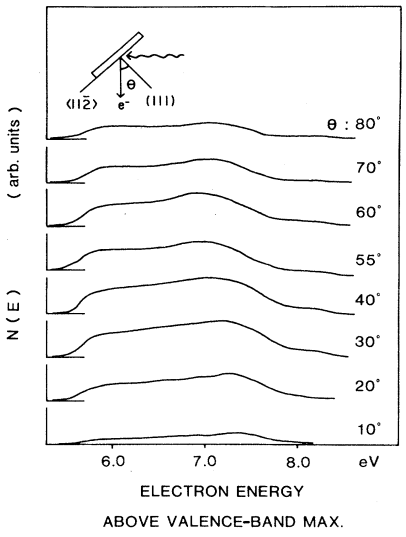

FIG. 4. Angle-resolved-photoemission spectra for the (111) crystal face of Si at $h\nu=7.75$ eV. Polar angle θ is varied from the surface normal towards the $\langle 11\bar{2}\rangle$ direction.

hibit broad structures which are insensitive to the angle θ. Figure 4 shows the spectra for the (111)-$\langle 11\bar{2}\rangle$ measurement for $h\nu=7.75$ eV. The spectra do not show strong peaks although there is some weak structure which changes with the angle θ. The rest of the broad structures are similar to those of Fig. 3.

Table I summarizes our measured results regarding the intensity of the peak at $h\nu=7.75$ eV for major crystal faces and directions. The strong peak is observed only for the (111)-$\langle 0\bar{1}1\rangle$, (100)-$\langle 0\bar{1}1\rangle$, and (100)-$\langle 001\rangle$ measurements which are indicated as "strong." The spectra for the latter two measurements are shown in Figs. 5 and 6, respectively. The spectra in other sets of measurements, indicated by "weak," show only the broad structures similar to those shown in Fig. 4.

IV. DISCUSSION

A. Energy-band dispersion and critical-point behavior

In the present photon-energy range the photoemission process may be described in terms of the direct optical transition in the bulk followed by transport to and escape through the surface.[16]

The experimental results described in Sec. III show that the peak in the photoemission spectra is enhanced only at a particular value of photon energy and particular directions of crystal face and photoemission. The strong peak is observed only for the (111)-$\langle 0\bar{1}1\rangle$, (100)-$\langle 0\bar{1}1\rangle$, and (100)-$\langle 001\rangle$ measurements. This fact indicates that the optical transition takes place mainly at a limited region of the wave vector and energy in the Brillouin zone. If the electron wave vector component $k_{||}$ parallel to the sample surface is conserved during the photoemission process, the electrons contributing to the (111)-$\langle 0\bar{1}1\rangle$ measurement must have their wave vector lying in the plane including $\langle 111\rangle$ and $\langle 0\bar{1}1\rangle$ axes. This plane contains highly symmetric directions such as Γ—L, Γ—K, and Γ—W. Similarly for the (100)-$\langle 0\bar{1}1\rangle$ and (100)-$\langle 001\rangle$ measurements, the electron wave vectors lie in the plane including the $\langle 100\rangle$ and $\langle 0\bar{1}1\rangle$ axes and $\langle 100\rangle$ and $\langle 001\rangle$ axes, respectively. The former plane contains Γ—K, Γ—L, Γ—U, and Γ—X, while the latter contains Γ—X, Γ—K, and Γ—W as highly symmetric directions. The direction common to these three planes is Γ—K. As listed in Table I the strong

TABLE I. Summary of the experimental result on the features of the peak at $h\nu=7.75$ eV. Some of the results correspond to the peaks in Figs. 3—6. Measurements are carried out for those combinations of the crystal face and direction which are perpendicular to each other. Other combinations not perpendicular to each other are left as blank.

Crystal face	Direction (tangential) ⟨100⟩	⟨001⟩	⟨0$\bar{1}$1⟩	⟨111⟩	⟨11$\bar{2}$⟩
(100)		strong	strong		
(011)	weak		weak		
(0$\bar{1}$1)	weak			weak	
(111)			strong		weak

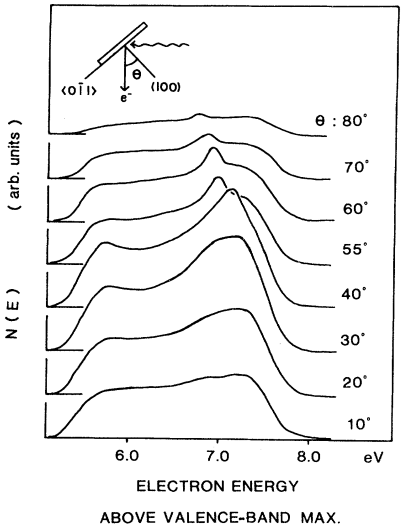

FIG. 5. Angle-resolved-photoemission spectra for the (100) crystal face of Si at $h\nu=7.75$ eV. Polar angle θ is varied from the surface normal towards the $\langle 0\bar{1}1\rangle$ direction.

peak is not observed for the (111)-$\langle 11\bar{2}\rangle$ measurement. Since the $\langle 11\bar{2}\rangle$ direction is, by symmetry, only 30° off from the $\langle 0\bar{1}1\rangle$ direction (Γ—K), the strong photoemission occurs closely along the Γ—K line. Hence the experimental results may be explained without contradiction if the observed peak is attributed to photoexcitations from a wave-vector space in the vicinity along Γ—K of the Brillouin zone.

The above interpretation is further supported in the detailed comparison of the spectra for the (111)-$\langle 0\bar{1}1\rangle$ and (100)-$\langle 0\bar{1}1\rangle$ measurements (Figs. 3 and 5). These spectra show that the peaks having the same energy for the two measurements appear at about the same angle θ. The observed photoelectrons in these spectra are excited in two

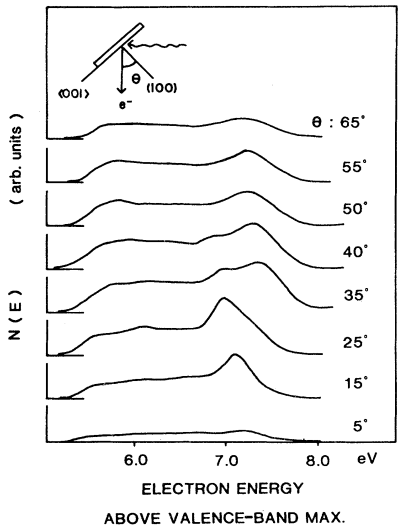

FIG. 6. Angle-resolved-photoemission spectra for the (100) crystal face of Si at $h\nu=7.75$ eV. Polar angle θ is varied from the surface normal towards the $\langle 001\rangle$ direction.

different planes in the Brillouin zone but have the same parallel component of $\vec{k}$ along the Γ—K direction. Hence the two measurements exhibit the same dependence for the final-state energy of electron E vs θ if the photoexcitation takes place along Γ—K. From E and θ, the value of $k_{||}$ is estimated to be about $\frac{1}{2}$ from Γ to K by the relation

$$k_{||}=\frac{[2m(E-\phi)]^{1/2}}{\hbar}\sin\theta\,, \tag{1}$$

where ϕ is the vacuum level relative to the top of the valence band. The above experimental observation shows that the strong peak found in the spectra arises from the photoelectrons excited near the midpoint along Γ—K.

Figure 7 shows the energy-band structure of Si calculated with the pseudopotential parameters determined by Nara and Kobayasi.[12,13] This energy-band calculation is adopted in our analysis since the pseudopotential including the nonlocal part are determined with a particular emphasis in obtaining the detailed structure of high-lying conduction bands up to 10 eV.[13] The strong peak ob-

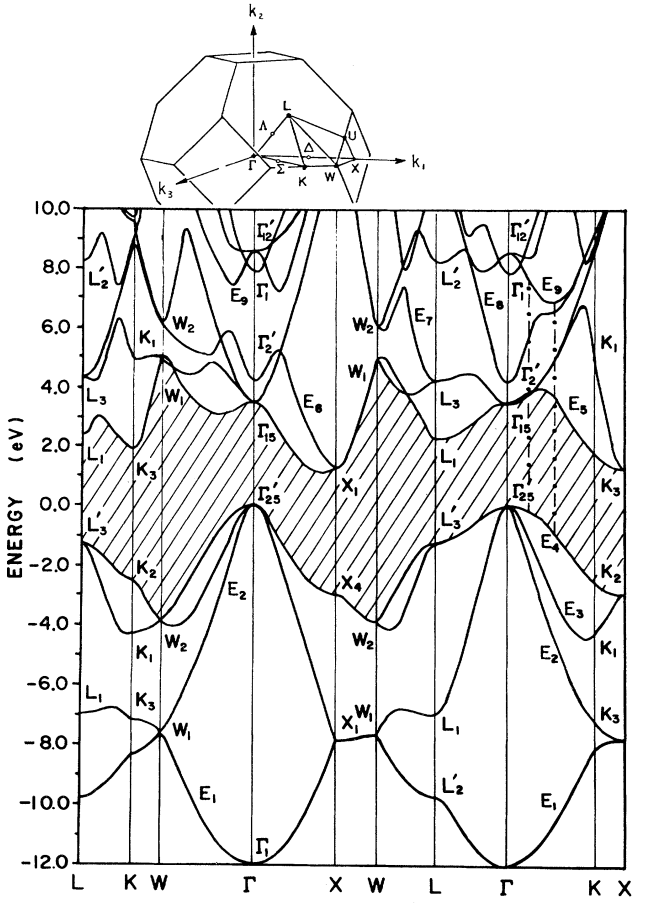

FIG. 7. Brillouin zone and the energy bands of Si along principal symmetry lines calculated with the pseudopotential parameters given by Nara and Kobayasi (Refs. 12 and 13). The forbidden gap, between the fourth band, E_4, and the fifth, E_5, is indicated by hatched area. Dashed-dotted lines along the Γ—K line represent possible optical transitions between the bands E_4 and E_9 at $h\nu=7.75$ eV.

served in the measurement at $h\nu=7.75$ eV occurs within the energy range 6.5—7.5 eV. The transition resulting in the final state of electrons in this energy range is the excitation from band E_4 (the highest valence band) to band E_9 (the fifth conduction band) at the Γ—K line as shown by dashed-dotted lines in Fig. 7. Since this pair of bands have similar dispersions near the midpoint on the Γ—K line, a high joint density of states may be expected for optical transition at $h\nu=7.75$ eV. It is also noted that in this region along the Γ—K line, the final-state energy E decreases with increase in $\vec{k}$. These facts explain qualitative features of the experimental observation discussed above.

To make detailed comparison with experiment, E vs $\vec{k}$ of the final state is calculated for the transition between bands E_4 and E_9. For the direct optical transition the energy and momentum conservations define the constant optical-energy surface in the $\vec{k}$ space for a given $h\nu$ (hereafter denoted as optical-energy surface),[5] while E defines the constant electron-energy surface of the final state. The intersection of the two surfaces gives theoretically predicted values of E and $\vec{k}$ of electrons contributing to the photoemission spectrum.

The results of E-vs-$\vec{k}$ calculations are plotted in Figs. 8(a), 8(b), and 8(c), for the Γ-K-W-L, Γ-K-L, and Γ-X-W-K planes, respectively. The solid lines originating from points α, β, and γ represent contours of the constant optical-energy surface for $h\nu=8.0$, 7.75, and 7.5 eV, respectively, and the dashed lines originating from points a—d are those of the constant electron-energy surface for $E=7.5$, 7.3, 7.1, and 6.9 eV, respectively. For our particular case the photon energy of the contour originating from β, denoted by "β line," corresponds to the incident-photon energy used in the measurements of Figs. 3, 5, and 6. As already inferred from the experimental observations, the calculation shows that the β line is located closely along the Γ—K line near its midpoint. The electron-energy contour intersects the β line at energies between 7.6 and 6.9 eV.

From the spectra shown in Figs. 3, 5, and 6, E and $k_{||}$ component parallel to the sample surface are determined experimentally from the peak energy and angle of photoelectrons using Eq. (1) with $\phi=5.07$ eV relative to the top of the valence band.[17] The results are represented by solid circles on the straight line at the bottom of each figure. The experimental points in Fig. 8(a) are deduced from the (111)-$\langle 0\bar{1}1\rangle$ measurement (Fig. 3) and are plotted on the line along the Γ—K direction since the electron emission in the (111)-$\langle 0\bar{1}1\rangle$ measurement comes from optical transition within the Γ-K-W-L plane and the electron wave-vector component $k_{||}$ parallel to the sample surface is in the direction of the Γ—K line. Similarly the experimental points in Fig. 8(b) are deduced from the (100)-$\langle 0\bar{1}1\rangle$ measurement (Fig. 5) and are plotted on the line along Γ—K. For Fig. 8(c) the experimental points are deduced from the (100)-$\langle 001\rangle$ measurement (Fig. 6) and are plotted on the line along Γ—X.

The agreement between theory and experiment may be examined by comparing the experimentally determined $k_{||}$ with the calculated $k_{||}$ evaluated at the point of intersection for the β line and the contour of electron energy corresponding to the measured peak energy. Thus, in Fig. 8(a), the value of $k_{||}=4.7\times10^7$ cm^{-1} for the peak at 7.1 eV is in good agreement with the calculated value of $k_{||}=5.4\times10^7$ cm^{-1} at the intersection of the β line ($h\nu=7.75$ eV) and contour c ($E=7.1$ eV). Similar results are obtained for Fig. 8(b). For Fig. 8(c) the (100)-$\langle 001\rangle$ measurement determines $k_{||}$ along the Γ—X direction which is about 45° off from the actual $\vec{k}$ direction. Hence the experimental $k_{||}$ must be compared with the calculated $\vec{k}$ at the intersection which is projected onto Γ—X. Accordingly the experimental points along Γ—X appear at

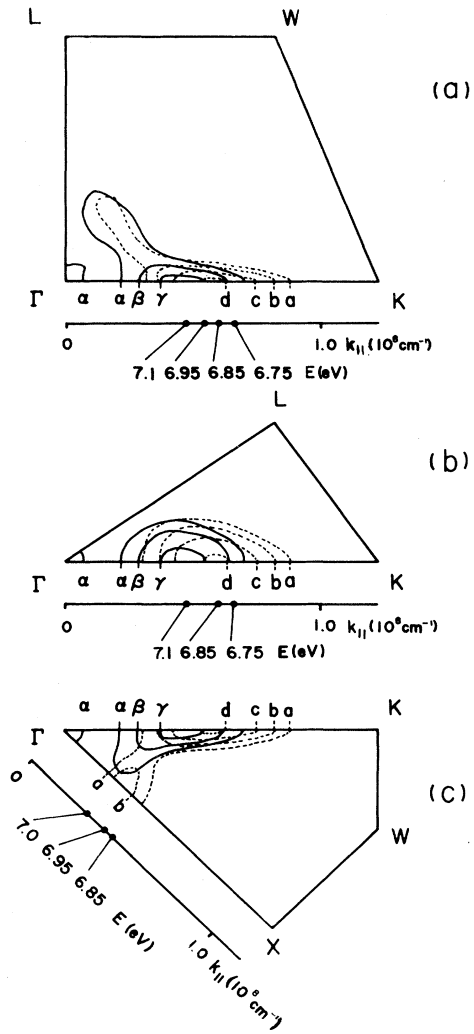

FIG. 8. Contours of constant photon energy (solid lines) for interband transition E_4—E_9 and constant electron energy (dashed lines) for the band E_9 in the planes of (a) Γ-K-W-L, (b) Γ-K-L, and (c) Γ-X-W-K. For each plane the photon energy $h\nu$ is represented by $\alpha=8.0$ eV, $\beta=7.75$ eV, and $\gamma=7.5$ eV, while the electron energy E is denoted by $a=7.5$ eV, $b=7.3$ eV, $c=7.1$ eV, and $d=6.9$ eV. For comparison the experimental points deduced from the spectra of Figs. 3, 5, and 6 are shown by solid circles on the straight line at the bottom of (a), (b), and (c), respectively. The numerical number expresses the electron energy E of the peak and the distance from the Γ point to the solid circle represents the magnitude of $k_{||}$ evaluated from E and θ using Eq. (1).

smaller values of $k_{||}$ (closer to the Γ point) as compared to the experimental points of Figs. 8(a) and 8(b). Consistent interpretation is obtained throughout the three kinds of measurements shown in Fig. 8.

In the (111)-$\langle 0\bar{1}1\rangle$ and (100)-$\langle 0\bar{1}1\rangle$ measurements (Figs. 3 and 5), the peak is observed clearly between $\theta=30°$ ($E=7.2$ eV) and 80° ($E=6.7$ eV). The calculation, on the other hand, predicts that the peak starts appearing at $\theta=21°$ ($E=7.6$ eV) and continues to appear up to $\theta=62°$ ($E=6.9$ eV). The upper and lower limits in angle come from the fact that the optical-energy contour β intersects the electron-energy contour at the value of $k_{||}$ between 2.7×10^7 and 6.9×10^7 cm^{-1}. These values of $k_{||}$ together with the corresponding electron energies give the above angle limits. It is difficult to determine experimentally at what angle and energy the peak starts appearing because the peak in the spectrum is rather broad at low angles of emission. The spectra do indicate, however, that the peak starts to appear at a finite value of θ around 30°. The broadening of the peak at those low angles may be explained in part in terms of the present calculation. As shown in Fig. 8, the optical-energy contour β near the intersection of electron contour a of 7.5 eV lies almost perpendicular to the Γ–K line. As a result the photoelectrons having different energies around 7.5 eV have nearly equal $k_{||}$ and hence emit in a narrow range of angle from the sample surface towards the electron analyzer. Because of a finite slit width of the electron analyzer the peak width in the spectrum becomes broadened for the energy around 7.5 eV.

B. Determination of local minimum for band E_9

From the quantitative consistency between theory and experiment, one may attempt to determine the local minimum of band E_9 by extending the measurements to the lower photon energies. At $h\nu=7.36$ eV, as shown in Fig. 9, the peak appears between $E=7.0$ ($\theta=30°$) and 6.6 eV ($\theta=65°$). At lower photon energies, the peak begins to diminish in the background spectrum, but its energy remains above 6.6 eV for any θ. Such photoelectron peaks become undetectable below $h\nu=7.3$ eV.

The above experimental observations may be interpreted in terms of an optical transition schematically shown in Fig. 9. For $h\nu=7.36$ eV, let optical transitions take place between $A\rightarrow A'$ through $B\rightarrow B'$. From the experiment the transition $A\rightarrow A'$ corresponds to the peak at $E=6.6$ eV ($\theta=65°$) so that, from Eq. (1), $k_{||}=5.6\times10^7$ cm^{-1} along Γ–K. The transition $B\rightarrow B'$ corresponds to $E=7.0$ eV ($\theta=30°$) with $k_{||}=3.5\times10^7$ cm^{-1}. For higher photon energies, such as for the spectrum shown in Fig. 3, $A\rightarrow A'$ moves to the right and $B\rightarrow B'$ to the left in accordance with the increase in the vertical energy separation. On the other hand, the decrease in $h\nu$ would shift $A\rightarrow A'$ and $B\rightarrow B'$ towards each other until they merge to $C\rightarrow C'$ which represents the minimum vertical energy difference between E_4 and E_9. The peak must disappear below the photon energy corresponding to $C\rightarrow C'$. In our measurement this photon energy is equal to $h\nu=7.3\pm0.1$ eV. The peak at $E=6.6$ eV ($\theta=65°$) observed for the photon energy at $h\nu=7.36$ eV is the lowest in electron energy throughout the measurement for $h\nu=7.3$–8.3 eV and corresponds, in this energy-band scheme, to the local minimum of band E_9 (point A'). Hence the spectra in Fig. 9 yield E and k of the local minimum along the Γ–K line to be

$$E=6.6\pm0.1\ ,$$

in eV, and

$$|\vec{k}|=(5.6\pm0.1)\times10^7\ ,$$

in cm^{-1}, while the band-structure calculation (Fig. 7) gives $E=6.88$ eV and $|\vec{k}|=5.8\times10^7$ cm^{-1}.

C. Spectral resolution and intensity in angle-resolved photoemission

As shown in Fig. 8, E vs $\vec{k}$ is experimentally determined for the wave vector lying in three different planes in the Brillouin zone. In these measurements, while E is determined in a unique manner, $\vec{k}$ is measured only for the component parallel to the sample surface. The wave vector $\vec{k}$ is uniquely determined if the components of $\vec{k}$ projected along two different crystal faces are measured. Hence, in principle, one may deduce with the present technique the position of critical points and their energy dispersion along any direction about the critical points. For example, if the experimental results for the (111)-$\langle 0\bar{1}1\rangle$ measurement are combined with the (0$\bar{1}$1)-$\langle 111\rangle$

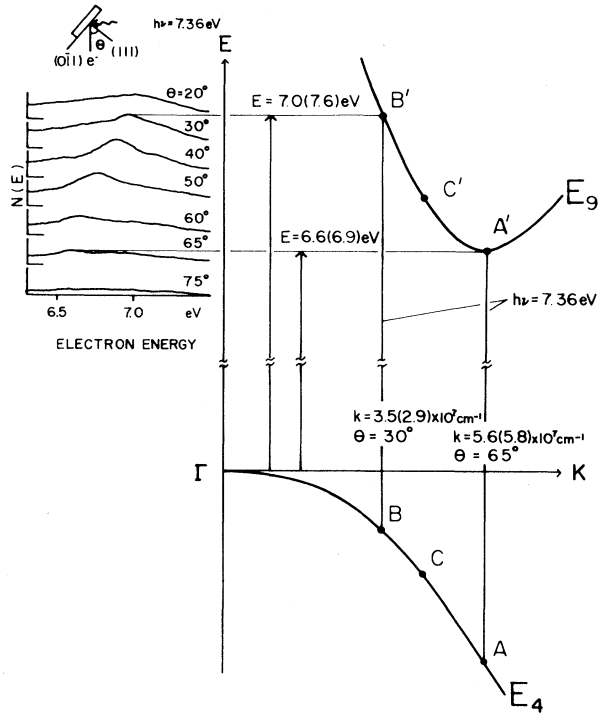

FIG. 9. Photoemission spectra measured at $h\nu=7.36$ eV and a schematic diagram representing the interpretation of the spectra in terms of the optical transition between the bands E_4 and E_9 taking place along the Γ–K line. In the diagram the values of E, θ, and k are deduced from the measurement. For comparison the calculated valus of E and k for $h\nu=7.75$ eV are shown in parentheses.

measurement, one may know E vs $\vec{k}$ around the local minimum of the band E_9 in the Γ-K-W-L plane [Fig. 8(a)]. In this particular case in Si, however, this type of analysis cannot be made since the $(0\bar{1}1)$-$\langle 111\rangle$ measurement does not exhibit strong structure in the spectrum as listed in Table I. As explained in the following paragraphs there are two reasons which prevent the appearance of the strong structure in the spectrum. One is due to the particular shape of the optical-energy surface and the other reason is related to the escape of photoelectrons to the vacuum.

As can be seen in the calculation of Fig. 8(a), the $(0\bar{1}1)$-$\langle 111\rangle$ measurements would determine E and $\vec{k}$ components parallel to Γ—L. The projection of β line onto Γ—L shows that photoelectron peaks between 6.9 and 7.6 eV appear within the range of angle $0\leq\theta\leq 5.1°$. As a result, peaks between 6.9 and 7.6 eV are superposed in the spectrum at $\theta\leq 5°$ and are observed only as a broad structure. Hence, E vs $\vec{k}$ along Γ—L cannot be determined from the $(0\bar{1}1)$-$\langle 111\rangle$ measurement. For the same reason E vs k along Γ—X in Fig. 8(b) cannot be determined from the $(0\bar{1}1)$-$\langle 100\rangle$ measurement (see Table I) which would provide the E-vs-$\vec{k}$ information in the Γ-K-L plane. For the Γ-X-W-K plane in Fig. 8(c), the (011)-$\langle 0\bar{1}1\rangle$ measurement combined with the (100)-$\langle 001\rangle$ would determine E vs $\vec{k}$. As listed in Table I, the (011)-$\langle 0\bar{1}1\rangle$ measurement also exhibits only a weak structure.

The reason for the lack of strong structure in the (011)-$\langle 0\bar{1}1\rangle$ measurement as well as other measurements in the (110) plane listed in Table I may be explained as follows: The final state of electrons inside the crystal is expressed in terms of a plane-wave expansion

$$\psi(\vec{k})=\sum_{\vec{G}} a_{\vec{G}}(\vec{k})\exp[i(\vec{k}+\vec{G})\cdot\vec{r}]\ , \tag{2}$$

where the sum is over the reciprocal-lattice vector $\vec{G}$ with $a_{\vec{G}}$ as the coefficient of each term. If each component is connected to the plane wave in vacuum with its amplitude proportional to $|a_{\vec{G}}(\vec{k})|^2$, the components having large $|a_{\vec{G}}(\vec{k})|^2$'s contribute dominantly to the photoemission.

The examination of the band-structure calculation shows that the band E_9 at points in $\vec{k}$ space discussed here has dominant coefficients for $\vec{G}\{200\}$ and $\vec{G}\{111\}$, and those for $\vec{G}\{220\}$ and others have at most 1 order of magnitude smaller values as shown in Table II. Accordingly, the photoemission is expected to be strong for the measurements in the (100) and (111) surfaces and weak for the (110) surface in agreement with the experimental observations.

TABLE II. Values of $|a_{\vec{G}}|^2$ for band E_9 at the local minimum along the Γ—K direction, $k=(0.375,0.375,0)$.

$\vec{G}\{hkl\}$	$\lvert a_{\vec{G}}\rvert^2$	$\vec{G}\{hkl\}$	$\lvert a_{\vec{G}}\rvert^2$
$\vec{G}\{\bar{1}11\}$	0.125	$\vec{G}\{202\}$	0.001
$\vec{G}\{200\}$	0.035	$\vec{G}\{\bar{2}02\}$	0.004
$\vec{G}\{\bar{2}00\}$	0.195	others	<0.001

According to the present discussion, the strong peak in the spectra is explained in terms of the direct optical-transition model. The rest of the structure in the spectra is rather broad and insensitive to the crystal face and the direction of electron emission. The band-structure calculation of Fig. 7 shows that there are other pairs of bands which contribute to the photoemission spectrum at $h\nu=7.75$ eV. A simple inspection of the band structure, however, indicates that most of the band pairs are expected to have low joint densities of states compared to the E_4 and E_9 pair. For some of these pairs, electrons are excited near the zone boundary and are totally reflected back into solid because their wave vector is too large to conserve both energy and momentum during the escape across the surface. Thus these band pairs contribute to photoemission spectra only as a weak and broad structure. Scattering by phonons may also broaden the structure, since for the photon-energy range used in our measurement the kinetic energies of photoexcited electrons lie in such a low range that the electron-phonon scattering is comparable to the electron-electron scattering.[18]

V. CONCLUSION

Angle-resolved-photoemission spectra on a single crystal of Si have been measured in the photon energy range 7.1—8.6 eV. The behavior of the pronounced peak is interpreted in terms of the direct transition model for the photoexcitation from the band E_4 to E_9 around the critical point along the Γ—K line. The analytical results are found consistent with the energy-band calculation of Nara and Kobayasi. This result shows that an arbitrary critical point structure may be studied in the photoemission spectrum by varying both the incident-photon energy and the detecting angle of photoelectrons. This type of analysis may be particularly effective for investigating the electronic structure of materials having complicated high-lying conduction bands, such as most of the group-IV semiconductors and III-V and II-VI compounds. The crystal potential for these compounds has not been determined accurate enough to ensure quantitative analysis of the band structure in the energy range over 20 eV from the bottom of the valence band. The reason is partly due to the lack of experimental data for this energy range of higher conduction bands. In comparison with the analytical methods published in the past,[19] the present approach would provide more realistic and reasonable parameters for the pseudopotential.

ACKNOWLEDGMENTS

The authors would like to thank Dr. S. Maekawa for valuable discussions and Mr. H. Kobayashi and Mr. Y. Tanno for their help in constructing the apparatus. They are grateful in particular to Professor H. Nara for his cooperation on the band-structure calculation. This work was supported by a Grant-in-Aid from the Ministry of Education, Science and Culture, Japan.

[1]See, for example, *Photoemission in Solids I,II,* edited by M. Cardona and L. Ley (Springer, Berlin, 1978).
[2]L. Ilver and P. O. Nilsson, Solid State Commun. 18, 677 (1976).
[3]G. V. Hansson and S. A. Flodström, Phys. Rev. B 17, 473 (1978).
[4]K. Furusawa, S. Suzuki, T. Sagawa, and T. Kobayasi, Jpn. J. Appl. Phys. 17, Suppl. 17-2, 225 (1978).
[5]E. O. Kane, Phys. Rev. 175, 1039 (1968).
[6]E. Dietz and D. E. Eastman, Phys. Rev. Lett. 41, 1974 (1978).
[7]R. Courths, Solid State Commun. 40, 529 (1981).
[8]N. E. Christensen, Solid State Commun. 38, 309 (1981).
[9]R. Courths, V. Badelier, and S. Hüfner, Solid State Commun. 38, 887 (1981).
[10]G. V. Hansson, R. I. G. Uhrberg, and S. A. Flodström, J. Vac. Sci. Technol. 16(5), 1287 (1979).
[11]D. E. Eastman, I. J. Himpsel, J. A. Knapp, and K. C. Pandey, in *Physics of Semiconductors, 1978,* edited by B. L. H. Wilson (IOP, Bristol, 1978), p. 1059.
[12]H. Nara and T. Kobayasi, J. Phys. Soc. Jpn. 41, 1429 (1976).
[13]The pseudopotential is expressed as a sum of a local part V_L containing three form factors and a nonlocal part V_{NL} containing two parameters. For V_{NL}, a Gaussian-type form,

$$V_{NL}=A_l\exp(-r^2/R_l^2)\,|\,l\rangle\langle\,l\,|\ ,$$

is adopted with $l=1$. These parameters for V_L and V_{NL} are interdependently determined so as to reproduce the various energy differences quoted from the previously published optical, UPS, and XPS data over the energy range of about 20 eV above the bottom of the valence band. The parameters thus determined, in Ry, are, for V_L, $V_L(111)=-0.2053$, $V_L(220)=0.0355$, and $V_L(311)=0.0724$; for V_{NL}, $2A_1=-5.7498$ with $R_1=0.7$ a.u. The relative rms deviation δ of the level fitting is obtained as $\delta=3.82\%$.
[14]C. C. Chang, Surf. Sci. 23, 283 (1970).
[15]J. E. Rowe, Phys. Lett. 46A, 400 (1974).
[16]P. J. Feibelman and D. E. Eastman, Phys. Rev. B 10, 2373 (1974).
[17]F. G. Allen and G. W. Gobeli, J. Appl. Phys. 35, 597 (1964).
[18]E. O. Kane, Phys. Rev. 159, 624 (1967).
[19]See, for example, M. L. Cohen, J. Phys. Soc. Jpn. 49, Suppl. A, 13 (1980). No discussion is given on the accuracy of band parameters for high-lying conduction bands.